K. GRUSZKA*,#, M. NABIAŁEK*, T. NOGA*

AB INITIO STUDY OF STRUCTURE, ELECTRONIC AND MAGNETIC PROPERTIES OF YFe₅ PHASE COMPOUND IN THE DFT FORMALISM

Paper presents results of studies on structural, electronic and magnetic properties of YFe₅ compound using density functional theory (DFT) approach. The GGA functional with ultrasoft pseudopotentials were used as implemented in Quantum Espresso software. The structure of YFe₅ compound was examined in three different states namely nonmagnetic, antiferromagnetic and ferromagnetic. Also two antiferromagnetic configurations were considered. From the total energy viewpoint the most likely ferromagnetic configuration is favorable. In order to achieve mentioned aims we present projected density of states, electronic band structure and Löwdin population analysis studies results.

Keywords: DFT, magnetism, electronic structure, structural parameters

1. Introduction

Ab initio design of materials is the subject of intense research made possible by using modern approaches such as density functional theory (DFT) studies. Using this method one can explore various material properties such as structural, electronic, magnetic, spectroscopic and mechanical [1-4]. This resulted in the possibility of low-level materials design taking into consideration of the individual atoms positions and their impact on macroscopic properties.

The RT_5 type compounds (where T is transition metal and R can be both transition metal or rare earth element) have drawn quite considerable interest because of their excellent permanent magnetic properties and the ability of changing properties with doping or different R element substitutions. As it is well known RT_5 type compounds crystallize in CaCu5 type structure where element R is located in 1a (0,0,0) position and T-type elements are taking other crystalline sites in respect to P6/mmm spacegroup presented by those materials [5]. It is worth noting that crystal structure of this type of compounds has very strong influence in determining both their magnetic and electronic properties.

The YFe₅ compound is a metastable phase which arises from high temperature decomposition of $Fe2Y_{17}$ phase also showing metastable character [6]. This rather complicated diffusion process is accompanied by formation of α-Fe phase which competes with emerging YFe₅ phase formation leading to its complete replacement with long time heat treatment. Small grains of this phase can be prepared by RF sputtering [5] or as shown in our previous work by special annealing process of amorphous iron based materials [7]. Some research of this and other types of similar compounds were previously published using extrapolation of experimental data [8] and FLAPW (full potential linearized augmented plane wave

method) method [9], the ASPW (augumented spherical plane wave) method [10]. As for our best knowledge none of this were conducted using ultrasoft pseudopotential (USPP) which is especially suited for treating metallic systems [11].

In this work we present ab initio studies of YFe₅ compound using density functional theory involving: structure optimization, projected density of states (PDOS), band structure calculations, magnetic and electronic properties and Löwdin population analysis.

2. Computational details

The YFe₅ phase crystallizes in hexagonal P6/mmm structure (no. 191). The primitive unit cell consists of 6 atoms (one Y and 5 Fe elements) and is presented in figure 1.
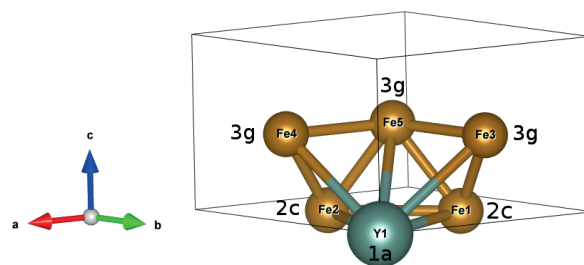

Figure 1. Structure of YFe5 primitive unit cell

Yttrium atoms are originated at (0,0,0) 1a position while Fe atoms are located in 2c (1/3,2/3,0) and 3g (1/2,0,1/2) sites. The three remaining Fe atoms are fixed by symmetry. All calculations were performed using plane wave basis set

* CZĘSTOCHOWA UNIVERSITY OF TECHNOLOGY, FACULTY OF PRODUCTION ENGINEERING AND MATERIALS TECHNOLOGY, INSTITUTE OF PHYSICS, 19 ARMII KRAKOWEJ AV.,42-200 CZĘSTOCHOWA, POLAND

Corresponding author: kgruszka@wip.pcz.pl

as implemented in Quantum Espresso software package [12]. For all calculations we used ultrasoft pseudopotentials with electronic configurations: [Ar] $4s^2$ $3d^6$ for iron with semicore states treated as valence with nonlinear core corrections and [Kr] $5s^2$ $4d^1$ for yttrium with nonlinear core corrections and s and p semicore electrons treated as valence [13]. The generalized gradient approximation (GGA) in the Perdew, Burke and Ernzerhof (PBE) form [14,15] was used as exchange-correlation energy. Spin polarization for magnetic Fe element was included to correctly account for its magnetic properties. Both PP's were prepared for scalar-relativistic calculations. For good convergence before any calculations we performed a series of tests for varying the wavefunctions kinetic energy cutoffs and k-points number with respect to total energy of system. Based on this tests we established plane wave kinetic energy cutoff *ecutwfc* to 60 Ry and kinetic energy cutoff for charge density *ecutrho* to 720 Ry for expansion of electronic functions. The k-point grid for Brillouin zone sampling and integration was set utilizing Monkhorst-Pack scheme [16] to 11x11x11 for x, y and z directions respectively. Further increase in both cutoffs and k-points number did not improved calculations significantly. In order to accelerate the system convergence a conventional Gaussian smearing of Fermi surface was adapted and set to 0.01 Ry. The energy convergence criteria was set to 10^{-7}.

Before any calculations the geometry optimization was done separately for ferromagnetic, antiferromagnetic and nonmagnetic structures and force convergence criteria for geometry optimization was set to 10^{-4}. The geometry optimization and ionic relaxation was done automatically using variable cell (vc-relax) algorithm utilizing Broyden–Fletcher–Goldfarb–Shanno (BFGS) quasi-Newton method under ambient (P=0) pressure [17]. This kind of optimization enables not only finding the lowest energy atomic positions inside cell but also is suitable for basic cell parameters refinement in terms of A,B,C, Cos(AB), Cos(AC) and Cos(BC) or lattice vectors. The starting lattice a parameter value was set to 9.505 Bohr in each magnetic case.

3. Results and discussion

As first the geometry optimization for nonmagnetic, ferromagnetic and antiferromagnetic configurations were made. In the ferromagnetic case a spin polarized calculation with collinear spins alignment along z-axis in uniform direction for every Fe atom was set. In this work we also considered two antiferromagnetic configurations. In the bulk crystal structure by looking on top of *ab* plane one can notice two corresponding layers of iron atoms forming two separate rings with yttrium atom in its center (fig. 2). The first considered antiferromagnetic configuration take into account that all top ring spins are up while bottom were set down, second configuration was reversed. The energy of those two configurations converged to the very same value (as expected by symmetry and periodicity of crystal structure) so in this sense they are equivalent.
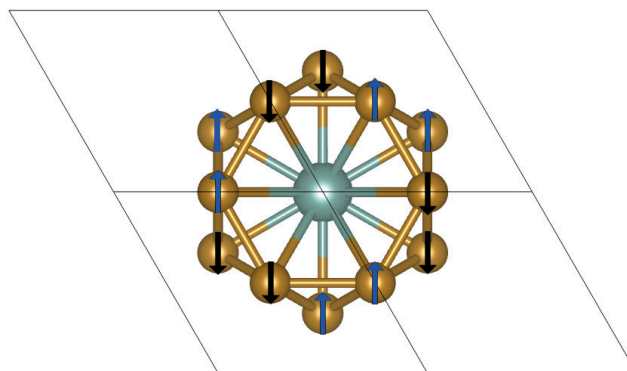

Fig 2. YFe₅ AFM configuration
Figure 2. The one of considered antiferromagnetic configurations seen by looking on the ab plane. The yttrium (light blue) atom is located in the middle. Arrows represent opposite spins

Data obtained from geometry optimization from all magnetic configurations are summarized in table 1.

As can be seen in Table 1, taking magnetization into account causes relatively significant changes especially in a,b and c lattice parameters. The cell volume rises about 8 $Å^3$ for FM state in comparison to non magnetic configuration and about 5.8 $Å^3$ For AFM state in comparison to non magnetic case.

Deformation also occurs in angles between the principal axes, the largest deviation in respect to the spacegroup was observed for the AFM configuration In general a good agreement can be seen in accordance both to previous calculations and experimental extrapolated and interpolated data.

After ionic relaxation of presented magnetic configurations the self consistent field calculation of total energy was calculated. From this calculation following energy values were obtained: NONMAG=-1333.66228836 Ry, AFM=

TABLE 1

Structural parameters for YFe5 from our calculation in comparison with other works

Configuration	a [Å]	b [Å]	c [Å]	α [°]	β [°]	γ [°]	V [Å3]
NONMAG.	4.8644	4.8638	3.8676	89.9997	90.0074	119.5047	79.6401
AFM	5.0113	5.0113	3.9280	90.0001	90.0001	121.1750	84.4378
FM	5.0775	5.0775	3.9267	90.0001	89.9996	120.0082	87.6671
FM GGA [5]	5.03	-*	3.87	-*	-*	-*	85.0
NONMAG. [5]	4.93	-*	3.80	-*	-*	-*	79.9
Exp. extrapol. FM [8]	5.03	-*	4.17	-*	-*	-*	91.4
Interpol. FM [8]	4.99	-*	4.03	-*	-*	-*	86.2

*- From P6/mmm spacegroup symmetry assuming: a=b and α=β=90°, γ=120°

-1333.73972913 Ry and FM= -1333.81363411 Ry. This result indicates that the most favorable magnetic configuration is the ferromagnetic case (in well accordance with experimental).

Next we calculated the band structure of YFe$_5$ compound along following high-symmetry lines: Γ→X→K→Z→B→Γ. The electronic band structure diagram is presented in figure 3.
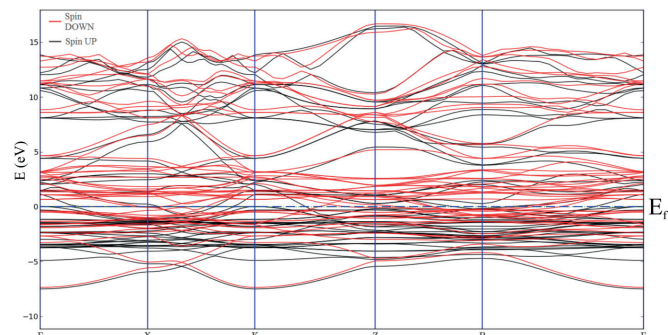

Figure 3. Electronic band structure diagram for ferromagnetic YFe$_5$. Black line indicates states with up spin, red lines are denoting states with spin down. Ef (blue dashed line) denotes for Fermi energy

Analysis of figure 3 shows that compound is fully metallic, showing no any band gaps. The bands derived from spin up (majority) and spin down (minority) components split apart due to exchange coupling between electrons (the red and black lines don't overlap) which is characteristic for ferromagnetic materials [18]. The calculated average splitting parameter value δE_Γ=0.68 eV reflects the strength of exchange between magnetic ions, with for comparison for bulk Fe is about δE_Γ=2 eV. The lowering of average splitting parameter δE_Γ by introduction of yttrium (and thus resulting in different crystal structure) may lead to decrease in Curie temperature as a consequence of decreasing magnetic moment in comparison to pure Fe. The calculations of band structure and average splitting parameter included 70 bands near the Fermi level (Ef).

Results of projected density of states calculations for studied phase in ferromagnetic configuration are shown in figures 4,5,6 and 7. The total dos (fig. 4) is a sum over all PDOS curves including one yttrium atom located at (1a) site, two Fe atoms from (2c) sites and three Fe atoms from (3g) sites. The x-axis zero mark denotes Fermi energy. In case of all plots (figs 4-7) positive values on y-axis (states/eV) are standing for spin up and negative values are spin down states.
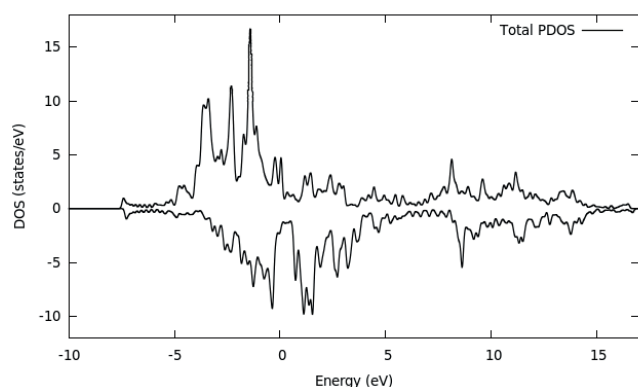

Figure 4 Total PDOS for YFe$_5$ ferromagnetic configuration. The zero energy is taken as Fermi level

As can be seen at the Fermi energy there is non-zero DOS again confirming the metallic character of compound.

In the following PDOS figures (5-7) only 4p, 5s and 4d in case of Y and 3p, 4s and 3d for both iron sites projected densities are shown. The calculated semicore (s, p) states are marginal to total PDOS.
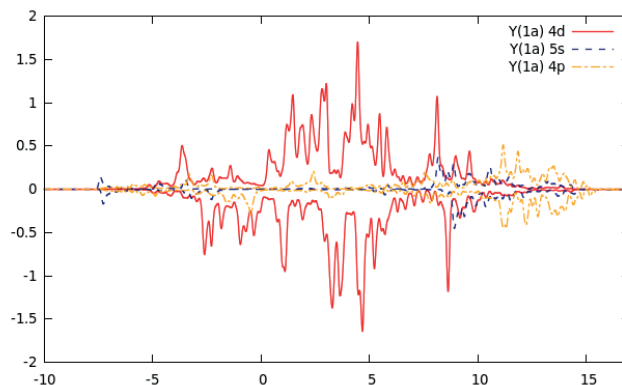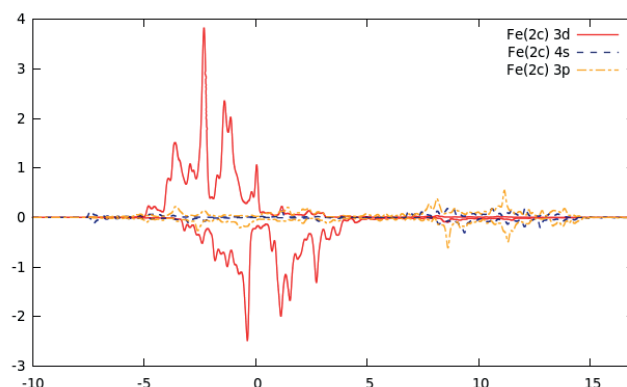

Figure 5. PDOS curves for Y(1a)

Figure 6. PDOS curves for Fe(2c)
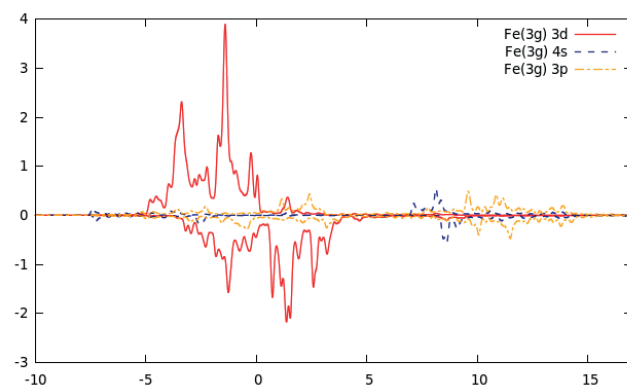
Figure 7. PDOS curves for Fe(3g)

In the case of yttrium 4d shell has the largest share both in the Fermi energy region as in overall. The 4p and 5s has low but non zero impact in this region. Yttrium 4d band is located mainly above Fermi energy, but in comparison to both iron sites it shows generally much even distribution in whole presented energy range. For the iron in both 2c and 3g sites the PDOS is dominated mainly by 3d electrons. The 3d bands seem to be located mostly below Fermi energy and the DOS at

372

the Fermi is clearly smaller but still significant. As can be seen in figs 6-7 the 3d electrons DOS above (but near) Fermi level is dominated by spin down configuration. PDOS for both iron sites below Fermi energy level that originate from 3s and 4s shells contributes very low to overall DOS and both together they contribute less than 5% in this region. Above Fermi energy level aiming toward higher energies this situation turn over and s and p electrons have now the main contribution in PDOS. Despite the different iron atom locations in the primary cell, the PDOS curves have similar character though of course

TABLE 2

Löwdin overlap population charges

Atom(site)	orbital spin up			orbital spin down		
Y(1a)	5s=1.0876	4p= 3.2130	4d=0.6608	5s=1.1303	4p= 3.3433	4d=1.1619
		px=1.0816	dxz=0.1068		px=1.1260	dxz=0.2036
		py=1.0576	dyz=0.0976		py=1.1073	dyz=0.1989
		pz=1.0738	dxy=0.1692		pz=1.1099	dxy=0.2581
			dz2=0.1347			dz2=0.2479
			dx2-y2=0.1524			dx2-y2= 0.2534
	polarization = -0.6740, s = -0.0427, p = -0.1303, d = -0.5010					
Fe1(2c)	4s=1.1608	3p=3.4004	3d=4.5283	4s=1.1775	3p=3.5221	3d=2.2088
		px=1.1376	dxz=0.8771		px=1.1916	dxz=0.5422
		py=1.1217	dyz=0.8789		py=1.1834	dyz=0.5389
		pz=1.1411	dxy=0.9381		pz=1.1471	dxy=0.3795
			dz2=0.8938			dz2=0.3450
			dx2-y2=0.9405			dx2-y2=0.4032
	polarization = 2.1811, s = -0.0167, p = -0.1217, d = 2.3195					
Fe2(2c)	4s=1.1608	3p=3.4004	3d=4.5283	4s=1.1775	3p=3.5221	3d=2.2083
		px=1.1375	dxz=0.8772		px=1.1916	dxz=0.5415
		py=1.1217	dyz=0.8787		py=1.1834	dyz=0.5394
		pz=1.1411	dxy=0.9381		pz=1.1471	dxy=0.3795
			dz2=0.8938			dz2=0.3449
			dx2-y2=0.9404			dx2-y2=0.4031
	polarization = 2.1815, s = -0.0167, p = -0.1217, d = 2.3200					
Fe3(3g)	4s=1.1696	3p=3.3683	3d=4.5563	4s=1.1889	3p=3.4927	3d=1.9373
		px=1.1060	dxz=0.9593		px=1.1687	dxz=0.2837
		py=1.1315	dyz=0.8688		py=1.1686	dyz=0.4485
		pz=1.1307	dxy=0.8959		pz=1.1553	dxy=0.4757
			dz2=0.8864			dz2=0.4343
			dx2-y2=0.9459			dx2-y2=0.2951
	polarization = 2.4754, s = -0.0192, p = -0.1244, d = 2.6190					
Fe4(3g)	4s=1.1731	3p=3.3864	3d=4.5616	4s=1.183	3p=3.5080	3d=2.0423
		px=1.1447	dxz=0.8948		px=1.1833	dxz=0.4434
		py=1.1125	dyz=0.9307		py=1.1681	dyz=0.3760
		pz=1.1292	dxy=0.9294		pz=1.1566	dxy=0.3561
			dz2=0.8843			dz2=0.4361
			dx2-y2=0.9225			dx2-y2=0.4306
	polarization = 2.3872, s = -0.0105, p = -0.1216, d = 2.5194					
Fe5(3g)	4s = 1.1714	3p=3.3656	3d=4.5531	4s=1.1924	3p=3.4874	3d=1.9422
		px=1.1417	dxz=0.8744		px=1.1786	dxz=0.4264
		py=1.0932	dyz=0.9486		py=1.1542	dyz=0.3074
		pz=1.1308	dxy=0.9208		pz=1.1546	dxy=0.3464,
			dz2=0.8846			dz2=0.4355
			dx2-y2=0.9247			dx2-y2=0.4264
	polarization = 2.4681, s = -0.0210, p = -0.1218, d = 2.6109					

it can't be concluded that there is no difference. The main difference in 3d shell is shift of majority states peak towards Fermi level (considering site change order from 2c to 3g) and opposite change in minority spins.

In each case, the yttrium and iron atom PDOS curves have asymmetrical character (in terms of majority and minority spin). This can have a quite considerable influence on some key properties like transport properties or tunneling, when bias voltage is applied. For better determination of this properties a further spin polarization studies should be conducted.

Next, we performed Löwdin population analysis and the calculated data are presented in Table 2. Total calculated charges for atoms in studied cell are: Y=10.5969, Fe1=15.9979, Fe2=15.9972, Fe3=15.7131, Fe4=15.8551, Fe5=15.7122. As can be seen from analysis of Table 2 (as well as from PDOS curves) there is an imbalance between spin up and spin down electrons resulting both from valence electronic configurations and existence of non spin-paired electrons as well as from the differences in Pauling electronegativity of yttrium (1.22) and iron (1.83). Because of this electronegativity difference electrons from yttrium should move slightly towards iron in both 2c and 3g sites. The yttrium 4d orbital electron is therefore exchanged with iron 3d orbital.. A slight shift of iron 4d electrons toward spin down configuration for 2c site in respect to 3g site is also observed.

As shows the analysis of table 2, for the both 2c and 3g iron sites 4s and 3p shells are evenly occupied by spin up and down configurations. It is also case of yttrium where 5s and 4p shells show similar occupations. The biggest deviations from equilibrium can be observed in 3d (iron) and 4d (yttrium) shells.

4. Conclusions

In this paper we obtained PDOS, electronic band structure and Löwdin charges for YFe_5 compound. The calculations showed that most stable magnetic form is ferromagnetic, which is also characterized by the biggest unit cell (from considered configurations). Band and PDOS calculations showed the metallic character of studied phase. The Fermi energy level is dominated by d shell electrons from yttrium and both iron sites.

4. REFERENCES

[1] W. Huang, X. Wang, X. Chen, W. Lu, L. Damewood, C.Y. Fong, J. Magn. Magn. Matter. **377**, 252 (2015).

[2] T. Kaczmarzyk, K. Dziedzic-Kocurek, I. Rutkowska, K. Dziliński, Nukleonika **60(1)**, 57 (2015).

[3] A.D. Davletshina, R.A. Yakshibaev, N.N. Bikkulova, Yu.M. Stepanov, L.V. Bikkulova, Solid state ionics, **257**, 29 (2014) .

[4] T. Morshedloo, M.R. Roknabadi, M. Behdani, Physica C, **509**, 1 (2015).

[5] F. A. Mohammad, S. Yehia, S. H. Aly, Physica B, **407**, 2486 (2012).

[6] K. Gruszka M. Nabiałek, K. Błoch, J. Olszewski, Nukleonika **60(1)**, 23 (2015).

[7] K. Gruszka, M. Nabiałek, K. Błoch, S. Walters, Int. J. Mater. Res. **106(7)**, 1862 (2015).

[8] F. Maruyama, H. Nagai, Y. Amako, H. Yoshie, K. Adachi, Physica B, **266**, 356 (1998).

[9] P. Larson, I. Mazin, D.A. Papaconstantopoulos, Phys. Rev. B. **69**, 134408 (2004).

[10] R. Coehoorn, Phys. Rev. B, **39**, 13072 (1989)

[11] R.A. Hansel, C.N. Brock, B.C. Paikoff, A.R. Tackett, D.G. Walker, Comp. Phys. Commun. **196**, 267 (2015).

[12] P. Giannozzi et. al, J. Phys.: Condens.Matter, **21**, 395502 (2009).

[13] D. Vanderbilt, Phys. Rev. B **41**, 7892 (1990).

[14] J. P. Perdew, K. Burke, M. Ernzerhof, Phys. Rev. Lett. **77**, 3865 (1996).

[15] J. P. Perdew, K. Burke, M. Ernzerhof, Phys. Rev. Lett. **78**, 1396 (1997).

[16] H.J. Monkhorst, J.D. Pack, Phys. Rev. B **13**, 5188 (1976).

[17] C.G. Broyden, J. Appl. Math. **6(1)**, 76 (1970).

[18] V. Cardoso Schwindt, M. Sandoval, J.S. Ardenghi, P. Bechthold, E. A. Gonzalez, P.V. Jasen, J. Magn. Magn. Matter. **389**, 73 (2015).